Investigating the effect of different carrier gases on plasma-assisted multi-walled carbon nanotube growth

U. Sharma[1], S. C. Sharma[1]

[1]*Department of Applied Physics, Delhi Technological University (DTU)*

Shahbad Daulatpur, Bawana Road, Delhi 110042, India.

E-mail: umangsharma2810@gmail.com, suresh321sharma@gmail.com

ABSTRACT

A model is developed consolidating the carbon nanotube (CNT) charging rate, the energy of all the plasma species, and the multi-walled carbon nanotube (MWCNT) growth rate owing to the surface and bulk diffusions and accumulation of particles on the catalyst nanoparticle surface. Using acetylene as the hydrocarbon source, we have compared the influence of distinctive carrier gases on the structure of CNT. The conclusion drawn from the results obtained were that while argon favors the growth of carbon nanotubes, ammonia and nitrogen contributes to diminishing the growth of carbon nanotubes. The work can be thought useful to serve to a better understanding of the growth of MWCNT in the plasma and to study their field emission applications.

I. INTRODUCTION

The plasma-aided CNT fabrication via plasma-enhanced chemical vapor deposition (PECVD) has many advantages over other techniques namely low-temperature growth, vertical and uniformly aligned growth, single-walled CNT (SWCNT) or multi-walled CNT (MWCNT), etc. [1-7]. Several groups have experimentally observed the effect of various carrier gases such as ammonia, nitrogen, argon on the growth of CNTs [2-7]. Through the developed theoretical model mentioned in Sec. II, we study the carrier gas effect on the MWCNT growth. The model consists of the dynamics of all the species present in the reactive plasma, and the CNT growth equation to examine the effect of carrier gases have on the MWCNT growth. The results are discussed in Sec. III and conclusion in Sec. IV.

II. MODEL

In the investigative model, following the detailed analysis done by Sharma *et al.* [8], we have considered a plasma composed of acetylene (C_2H_2) as the hydrocarbon source gas; ammonia (NH_3), nitrogen (N_2), and argon (Ar) are different carrier gases, respectively. The reactive plasma

consists of electrons, neutrals, and ions of acetylene denoted as type A, and carrier gas (namely NH_3, N_2, and Ar) denoted as type B in the present study. All the terms have their usual notations [8].

$$\partial_\tau(n_e) = \sum_j \beta_j n_j - \sum_j \alpha_j n_e n_{ij} - \gamma_e \frac{n_{CNT}}{\lambda_s}\left(\begin{matrix}tip\\ e\end{matrix}\xi + \begin{matrix}cyl\\ e\end{matrix}\xi\right) - \mathrm{K}^{e}_{wall} n_e, \quad (1)$$

The first term of Eq. (1) represents the rise in electron density via ionization of neutrals, the second term denotes decrease due to recombination of electron and ions, the third term represents decrease owing to their accumulation at the MWCNT surface, and the discharge loss to the walls of the chamber is denoted lastly.

$$\partial_\tau(n_{iA}) = \beta_A n_A - \alpha_A n_e n_{iA} - \frac{n_{CNT}}{\lambda_s}\left(\begin{matrix}tip\\ iA\end{matrix}\xi + \begin{matrix}cyl\\ iA\end{matrix}\xi\right) + \sum_{\ell AB} k_\ell n_A n_{iB} - \sum_{qBA} k_q n_B n_{iA} - \mathrm{K}^{iA}_{wall} n_{iA} + \left(\frac{P}{E^{diss}_{CH} V}\right), \quad (2)$$

$$\partial_\tau(n_{iB}) = \beta_B n_B - \alpha_B n_e n_{iB} - \frac{n_{CNT}}{\lambda_s}\left(\begin{matrix}tip\\ iB\end{matrix}\xi + \begin{matrix}cyl\\ iB\end{matrix}\xi\right) + \sum_{qBA} k_q n_B n_{iA} - \sum_{\ell AB} k_\ell n_A n_{iB} - \mathrm{K}^{iB}_{wall} n_{iB} + \left(\frac{P}{E^{diss}_{H} V}\right), \quad (3)$$

In Eqs. (2) and (3), first term denotes the elevates the ion density because of dissociation of neutrals, next term denotes the dissipation due to recombination of ions with electrons, third term represents the loss due to their accumulation at the MWCNT surface; the ion-neutral reactions are incorporated in the fourth and fifth terms, sixth terms denotes the discharge loss to the walls and the last term incorporates the dissociation by plasma power.

$$\begin{aligned}\partial_\tau(n_A) = {} & \alpha_A n_e n_{iA} - \beta_A n_A + \frac{n_{CNT}}{\lambda_s}\left(1-\gamma_{iA}\right)\left(\begin{matrix}tip\\ iA\end{matrix}\xi + \begin{matrix}cyl\\ iA\end{matrix}\xi\right) - \frac{n_{CNT}}{\lambda_s}\gamma_A\left(\begin{matrix}tip\\ A\end{matrix}\xi + \begin{matrix}cyl\\ A\end{matrix}\xi\right) \\ & + \mathrm{Q}^{IF}_A - \mathrm{Q}^{OF}_A - \sum_{lBA} k_l n_A n_{iB} + \sum_{qAB} k_q n_B n_{iA} - J^{adsp}_A + J^{desp}_A - \mathrm{K}^{A}_{wall} n_A, \end{aligned} \quad (4)$$

$$\begin{aligned}\partial_\tau(n_B) = {} & \alpha_B n_e n_{iB} - \beta_B n_B + \frac{n_{CNT}}{\lambda_s}\left(1-\gamma_{iB}\right)\left(\begin{matrix}tip\\ iB\end{matrix}\xi + \begin{matrix}cyl\\ iB\end{matrix}\xi\right) - \frac{n_{CNT}}{\lambda_s}\gamma_B\left(\begin{matrix}tip\\ iB\end{matrix}\xi + \begin{matrix}cyl\\ iB\end{matrix}\xi\right) \\ & + \mathrm{Q}^{IF}_B - \mathrm{Q}^{OF}_B - \sum_{qBA} k_q n_B n_{iA} + \sum_{\ell AB} k_\ell n_A n_{iB} - J^{adsp}_B + J^{desp}_B + J_{thd} - \mathrm{K}^{B}_{wall} n_B, \end{aligned} \quad (5)$$

In Eqs. (4) and (5), first term descibes the rise in neutral density due to the ion-electron recombination, next term denotes the dissipation due to dissociation of neutrals the rise in neutral atom density due to ion neutralizationis descibed in third term, the fourth term characterizes the dissipation due to neutral atom accumulation at the MWCNT surface, the neutral plasma species

influx and outflux is denoted by the fifth and sixth terms, the neutral-ion reactions are incorporated in the seventh and eighth terms, ninth and tenth term represents the adsorption and desorption of neutrals onto/from the catalyst. The eleventh term of Eq. (5) indicates an increase in hydrogen species density due to the thermal de-hydrogenation process. The ending terms both equations signify the discharge loss.

$$\partial_\tau \left(N_g \right) = \left[D_s + D_b + 2\pi\kappa v r^2 \right] \times n_C S - n_{cg} S, \qquad (6)$$

The first term of Eq. (6) signifying the rate of cylindrical graphitic shell formation [9] denotes surface diffusion over catalyst surface, the second term denotes bulk diffusion through the catalyst, the third term incorporates the C-atom precipitation around the catalyst rear end forming cylindrical shells where n_C is the number density of carbon species on the catalyst nanoparticle [8] and, the last term denotes etching effects of the carrier gas species where *S* is the surface area of catalyst nanoparticle.

III. RESULTS AND DISCUSSION

The Eqs. (1-6) have been solved simultaneously for a typical glow discharge plasma parameter with the initial boundary conditions at $\tau = 0$ as mentioned in the work of Sharma *et al.* [8]. The variation of the carbon number density and number of graphitic shells for the MWCNT with time for different carrier gases is illustrated in Figs. 1 and 2, respectively. The observations drawn from the results are discussed alongside.

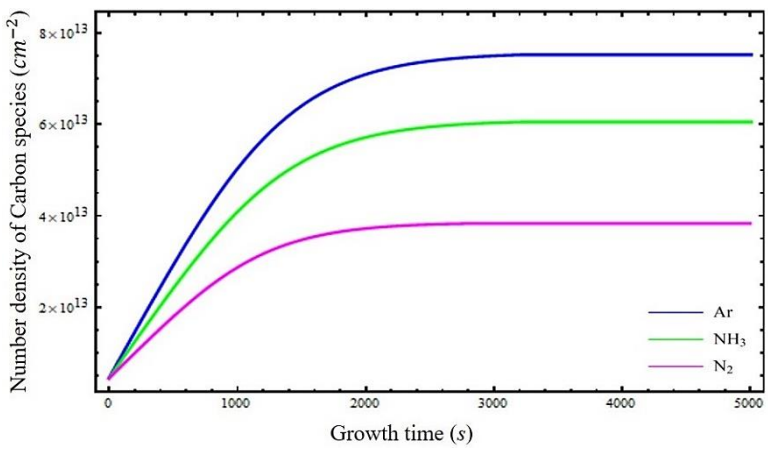

Figure 1. Time progression of carbon number density on catalyst particle.

The dissociation of hydrocarbon species, increases the number density of carbon species on the catalyst nanoparticle. This Carbon number density is higher for Ar compared to NH_3 and N_2, hence it would offer better MWCNT growth compared to others, as shown in Fig 1.

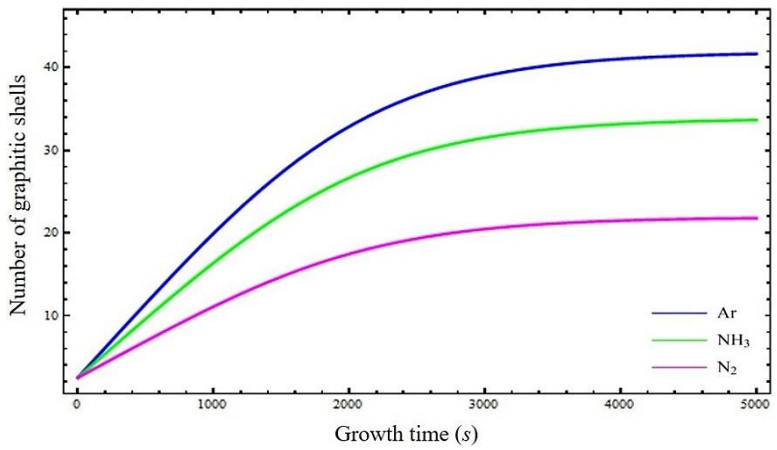

Figure 2. Time progression of graphitic shells of MWCNT.

As in case of Ar, the carbon number density is higher, so the number of cylindrical graphitic shells formed in this case are more compared to NH_3 and N_2, as shown in Fig 2. This increase in number of shells increases the radius of MWCNT, consequently, Ar offers a better MWCNT growth than NH_3 and N_2.

IV. CONCLUSION

The dynamics of the plasma species and MWCNT growth has been studied using the developed model incorporating the effects of various gases in plasma-assisted CNT growth process. The effect of gases; ammonia (NH_3), nitrogen (N_2), and argon (Ar) on the growth of the MWCNT are investigated. These results are in compliance with various experimental results [2-7]. The study can be proved valuable in the understanding of the use of CNT as field emitter devices.

ACKNOWLEDGEMENT

The authors are thankful to the Department of Science and Technology (DST), Government of India for providing the financial assistance under INSPIRE Fellowship.

REFERENCES

[1] S. Iijima, Nature **354,** 56 (1991).

[2] V. I. Merkulov, A. V. Melechko, M. A. Guillorn, D. H. Lowndes, and M. L. Simpson, Appl. Phys. Lett. **79,** 2970 (2001).

[3] W. Mi, J. Y. Lin, Q. Mao, Y. Li, and B. Zhang, J. Natural Gas Chem. **14,** 151 (2005).

[4] S. M. Toussi, A. Fakhru'l-Razi, A. L. Chuah, and A. R. Suraya, Sains Malays. **40,** 197 (2011).

[5] M. Jung, K. Y. Eun, J.-K. Lee, Y.-J. Baik, K.-R. Lee, and J. W. Park, Diamond Relat. Mater. **10,** 1235 (2001).

[6] W. Mi, J. Y. Lin, Q. Mao, Y. Li and B. Zhang, J. Nat. Gas Chem. **14,** 151 (2005).

[7] V. Kayastha, Y. K. Yap, S. Dimovski, and Y. Gogotsi, Appl. Phys. Lett. **85,** 3265 (2004).

[8] U. Sharma and S. C. Sharma, Physics of Plasmas **25,** 103509 (2018).

[9] R. Gupta, N. Gupta and S. C. Sharma, Physics of Plasmas **25,** 043504 (2018).